

Quantum Dot as a Spin-Current Diode

F. M. Souza,^{1,2} J. C. Egues,³ and A. P. Jauho⁴

¹ Instituto de Estudos Superiores da Amazônia, 66055-260, Belém, Pará, Brazil

² Grupo de Física de Materiais da Amazônia, Departamento de Física,
Universidade Federal do Pará, 66075-110, Belém, Pará, Brazil

³ Departamento de Física e Informática, Instituto de Física de São Carlos,
Universidade de São Paulo, 13560-970, São Carlos, São Paulo, Brazil

⁴ MIC - Department of Micro and Nanotechnology, NanoDTU,
Technical University of Denmark, Ørsted Plads, Bldg. 345E, DK-2800 Kgs. Lyngby, Denmark

(Date: December 2, 2024)

We report a study of spin dependent transport in a system composed of a quantum dot coupled to a normal metal lead and a ferromagnetic lead (NM-QD-FM). We use the master equation approach to calculate the spin-resolved currents in the presence of an external bias and an intra-dot Coulomb interaction. We find that for a range of positive external biases (current flow from the normal metal to the ferromagnet) the current polarization $\varphi = (I_{\uparrow} - I_{\downarrow})/(I_{\uparrow} + I_{\downarrow})$ is suppressed to zero, while for the corresponding negative biases (current flow from the ferromagnet to the normal metal) φ attains a relative maximum value. The system thus operates as a rectifier for spin-current polarization. This effect follows from an interplay between Coulomb blockade and nonequilibrium spin accumulation in the dot. In the parameter range considered, we also show that the above results can be obtained via nonequilibrium Green functions within a Hartree-Fock type approximation.

PACS numbers: PACS number

I. INTRODUCTION

Polarized transport in spin-dependent nanostructures is a subject of intense study in the emerging field of spintronics,¹ due to its relevance to the development of novel spin-based devices.^{2,3,4} In addition, transport through QDs provides information about fundamental physical phenomena in spin-dependent and strongly correlated systems, such as the Kondo effect,^{5,6,7,8,9} the Coulomb- and spin-blockade effects,^{10,11,12,13,14} tunnelling magnetoresistance (TMR),^{15,16,17,18,19,20,21,22,23} etc. Novel spin filters and pumps have also been proposed using QDs coupled to normal metal leads.^{24,25,26} A system of particular interest in this context comprises a quantum dot or a metallic grain coupled to ferromagnetic leads. The ferromagnetism of the leads introduces spin-dependent tunneling rates between the leads and the central region. This results in a nonzero net spin in the central region for asymmetric magnetization geometries. This effect is called spin accumulation or spin imbalance.^{27,28} It has been shown that spin accumulation affects several transport properties, such as magnetoresistance,^{18,31} (negative) differential resistance^{10,31} and the zero-bias anomaly.^{8,11,18} In addition it provides a way to generate and control the current spin polarization via gates or bias voltages,^{29,30} which is one of the main goals within spintronics.

Systems composed of a nonmagnetic lead and a ferromagnetic lead with a quantum dot or a quantum wire as spacer have been analyzed recently. It was pointed out that if the spacer is a dot and the ferromagnetic lead is half-metallic, a novel mesoscopic current-diode effect arises.^{4,31,32} Spin-current rectification was also predicted in an asymmetric system composed of a ferromagnetic (Fe or Ni) and nonmagnetic (Au or Pd) contacts coupled

to each other via a molecular wire.³³ Additionally, it was pointed out that a NM-QD-FM system can operate as a spin-filter and spin-diode.³⁴ In Ref. [34] the authors use the bias voltage to change the resonance position of the dot level with respect to the spin-split density of states of the ferromagnetic lead. This gives rise to spin-dependent currents.

Here we study spin-resolved currents in a single-level quantum dot attached to a nonmagnetic lead (“left lead”) and to a ferromagnetic lead (“right lead”), Fig. 1. As we shall show, the magnetic asymmetry between the left and right terminals results in a rectification of the current polarization when the system operates in the Coulomb blockade regime. More precisely, when the nonmagnetic lead operates as an emitter and the ferromagnetic lead as a collector, defined as the positive bias, the current is unpolarized. In contrast, when the ferromagnetic lead is the emitter and the nonmagnetic lead is the collector (negative bias) a polarized current arises. Importantly, this rectification occurs only in the Coulomb blockade regime, as we shall demonstrate both analytically and numerically. This is attributed to an interplay between nonequilibrium spin accumulation and Coulomb interaction within the dot. For bias values not in the Coulomb blockade regime, the current polarization found is essentially symmetric with respect to the bias, and no rectification is found.

In the main body of the text we employ the master-equation approach of Glazman and Matveev³⁵ to describe the spin-dependent transport through our NM-QD-FM junction in the regime $\Gamma_0 \ll k_B T$,³⁵ where Γ_0 is a characteristic tunneling rate. An alternative description in terms of nonequilibrium Green functions is also presented in the appendix. By performing a Hartree-Fock type factorization of the correlation functions in this nonequilib-

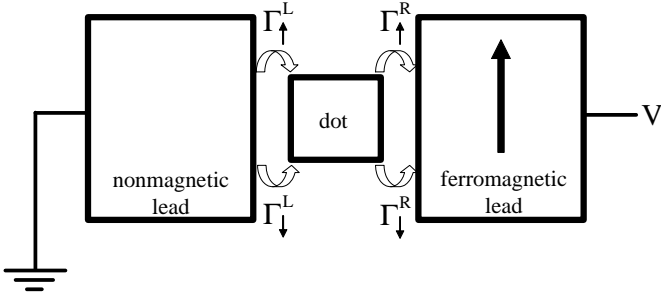


FIG. 1: System studied: a nonmagnetic quantum dot coupled via tunneling barriers to a nonmagnetic left lead and a ferromagnetic right lead. A bias voltage eV is applied across the system so that the left (μ_L) and right (μ_R) chemical potentials differ by $\mu_L - \mu_R = eV$.

rium formulation it is possible to obtain equivalent results to those of the master equation approach.

II. MODEL AND MASTER EQUATION APPROACH

The NM-QD-FM system we study is schematically illustrated in Fig. 1. An external bias voltage V drives the system away from equilibrium thus imposing a chemical potential imbalance between the left (L) and the right (R) leads: $\mu_L - \mu_R = eV$, where $\mu_{L(R)}$ is the chemical potential of the lead $L(R)$ and e is the absolute value of the electron charge ($e > 0$). The system Hamiltonian is

$$H = \sum_{\mathbf{k}\sigma\eta} \epsilon_{\mathbf{k}\sigma\eta} c_{\mathbf{k}\sigma\eta}^\dagger c_{\mathbf{k}\sigma\eta} + \sum_{\sigma} \epsilon_d d_\sigma^\dagger d_\sigma + U d_\uparrow^\dagger d_\uparrow d_\downarrow^\dagger d_\downarrow + \sum_{\mathbf{k}\sigma\eta} (t_{\mathbf{k}\sigma\eta} c_{\mathbf{k}\eta}^\dagger d_\sigma + t_{\mathbf{k}\eta}^* d_\sigma^\dagger c_{\mathbf{k}\sigma\eta}), \quad (1)$$

where $\epsilon_{\mathbf{k}\sigma\eta}$ is the free-electron energy with wave vector \mathbf{k} and spin σ in lead η ($\eta = L, R$), ϵ_d is the spin-degenerate dot level, U is the on-site Coulomb repulsion and the operators $c_{\mathbf{k}\sigma\eta}$ ($c_{\mathbf{k}\sigma\eta}^\dagger$) and d_σ (d_σ^\dagger) destroy (create) an electron with spin σ in the lead η and in the dot, respectively. The matrix element $t_{\mathbf{k}\sigma\eta}$ gives the lead-dot coupling. We do not consider any spin-flip processes.

To calculate the current we use rate equations,^{23,35} which yield

$$I_\sigma^\eta = e[\Gamma_{01\sigma}^\eta(1 - n_\sigma - n_{\bar{\sigma}}) - \Gamma_{10\sigma}^\eta n_\sigma + \tilde{\Gamma}_{01\sigma}^\eta n_{\bar{\sigma}}], \quad (2)$$

where we have assumed $\hbar = 1$. The parameter $\Gamma_{01\sigma}^\eta$ corresponds to the rate of adding an electron to the dot coming from lead η , and $\Gamma_{10\sigma}^\eta$ is the rate of moving one electron from the dot to lead η . In addition, $\tilde{\Gamma}_{01\sigma}^\eta$ gives the rate of moving one electron from lead η to the dot when it already has an electron with spin σ . The dot occupation $n_{\sigma(\bar{\sigma})}$ ($\bar{\sigma} = -\sigma$) is the probability of having one electron in the dot with spin σ ($\bar{\sigma}$). The tunneling rates are

$$\Gamma_{01\sigma}^\eta = \Gamma_\sigma^\eta f_\eta \quad (3)$$

$$\Gamma_{10\sigma}^\eta = \Gamma_\sigma^\eta (1 - f_\eta) \quad (4)$$

$$\tilde{\Gamma}_{01\sigma}^\eta = \Gamma_\sigma^\eta \tilde{f}_\eta, \quad (5)$$

where $f_\eta = 1/\{\exp[(\epsilon_d - \mu_\eta)/(k_B T)] + 1\}$ and $\tilde{f}_\eta = 1/\{\exp[(\epsilon_d + U - \mu_\eta)/(k_B T)] + 1\}$. The rates Γ_σ^η are related to the spin-resolved density of states of lead η via $\Gamma_\sigma^\eta = 2\pi|t|^2\rho_{\sigma\eta}(\epsilon)$. Here we assume $\Gamma_\uparrow^L = \Gamma_\downarrow^L$ and $\Gamma_\uparrow^R \neq \Gamma_\downarrow^R$. This reflects the fact that the density of states of the left lead is spin-degenerate while the right one is spin-split.

To calculate the current via Eq. (2) we need to find n_σ from²³

$$\frac{d}{dt} n_\sigma = \Gamma_{01\sigma}[1 - n_\sigma - n_{\bar{\sigma}}] - \Gamma_{10\sigma} n_\sigma + \tilde{\Gamma}_{01\sigma} n_{\bar{\sigma}}, \quad (6)$$

where

$$\Gamma_{01\sigma} = \Gamma_{01\sigma}^L + \Gamma_{01\sigma}^R = \Gamma_\sigma^L f_L + \Gamma_\sigma^R f_R \quad (7)$$

$$\Gamma_{10\sigma} = \Gamma_{10\sigma}^L + \Gamma_{10\sigma}^R = \Gamma_\sigma^L (1 - f_L) + \Gamma_\sigma^R (1 - f_R) \quad (8)$$

$$\tilde{\Gamma}_{01\sigma} = \tilde{\Gamma}_{01\sigma}^L + \tilde{\Gamma}_{01\sigma}^R = \Gamma_\sigma^L \tilde{f}_L + \Gamma_\sigma^R \tilde{f}_R. \quad (9)$$

In the stationary regime (i.e., $dn_\sigma/dt = 0$), Eq. (6) reduces to

$$n_\sigma = \frac{\Gamma_{01\sigma} + (\tilde{\Gamma}_{01\sigma} - \Gamma_{01\sigma})n_{\bar{\sigma}}}{\Gamma_{01\sigma} + \Gamma_{10\sigma}}, \quad (10)$$

which can be solved for each spin component, thus resulting in

$$n_\sigma = \frac{\Gamma_{01\sigma}\Gamma_{10\bar{\sigma}} + \Gamma_{01\bar{\sigma}}\tilde{\Gamma}_{01\sigma}}{\Pi_\sigma} \quad (11)$$

where $\Pi_\sigma = (\Gamma_{01\sigma} + \Gamma_{10\sigma})(\Gamma_{01\bar{\sigma}} + \Gamma_{10\bar{\sigma}}) - (\tilde{\Gamma}_{01\sigma} - \Gamma_{01\sigma})(\tilde{\Gamma}_{01\bar{\sigma}} - \Gamma_{01\bar{\sigma}})$. Hence the current becomes

$$I_\sigma^\eta = e \frac{\Gamma_{01\sigma}^\eta (\Gamma_{10\sigma}\Gamma_{10\bar{\sigma}} - \tilde{\Gamma}_{01\sigma}\tilde{\Gamma}_{01\bar{\sigma}}) - \Gamma_{10\sigma}^\eta (\Gamma_{01\sigma}\Gamma_{10\bar{\sigma}} + \Gamma_{01\bar{\sigma}}\tilde{\Gamma}_{01\sigma}) + \tilde{\Gamma}_{01\sigma}^\eta (\Gamma_{01\sigma}\Gamma_{10\sigma} + \Gamma_{01\bar{\sigma}}\tilde{\Gamma}_{01\bar{\sigma}})}{\Pi_\sigma} \quad (12)$$

Using Eq. (12) we can readily evaluate the current polarization $\varphi = (I_\uparrow - I_\downarrow)/(I_\uparrow + I_\downarrow)$. Next (Sec. III) we provide some simple analytic results valid in the Coulomb blockade regime. Numerical results are presented in Sec. IV.

III. COULOMB BLOCKADE REGIME

As we shall see, the most interesting behavior takes place in the Coulomb blockade (CB) regime. Here we give analytic expressions for the dot occupations, current, and its polarization in this regime. In the CB we have $\tilde{f}_\eta = 0$, since $\epsilon_d + U$ is well above μ_η . In addition if $\epsilon_d < \mu_L$ for $eV > 0$, or $\epsilon_d < \mu_R$ for $eV < 0$ we have $f_L = 1$, $f_R = 0$ or $f_L = 0$, $f_R = 1$, respectively. With these assumptions Eq. (11) reduces to

$$n_\sigma = \frac{\Gamma_\sigma^\eta \Gamma_{\bar{\sigma}}^{\bar{\eta}}}{\Gamma_\sigma^\eta \Gamma_{\bar{\sigma}}^{\bar{\eta}} + \Gamma_\sigma^L \Gamma_{\bar{\sigma}}^R + \Gamma_{\bar{\sigma}}^L \Gamma_\sigma^R}, \quad (13)$$

where $\eta = L$, $\bar{\eta} = R$ for $eV > 0$ and $\eta = R$, $\bar{\eta} = L$ for $eV < 0$. The current of the left lead then becomes

$$I_\sigma^L = \pm e \frac{\Gamma_\sigma^\eta \Gamma_{\bar{\sigma}}^L \Gamma_{\bar{\sigma}}^R}{\Gamma_\sigma^\eta \Gamma_{\bar{\sigma}}^{\bar{\eta}} + \Gamma_\sigma^L \Gamma_{\bar{\sigma}}^R + \Gamma_{\bar{\sigma}}^L \Gamma_\sigma^R} \quad (14)$$

where $\eta = R$ and the + sign corresponds to $eV > 0$, while $\eta = L$ and the - sign to $eV < 0$. The right side current is simple given by $I_\sigma^R = -I_\sigma^L$ for a spin-conserving stationary regime. Eq. (14) gives the (bias-independent) current in the CB regime. For the particular case of spin-independent tunneling rates, i.e., $\Gamma_\sigma^L = \Gamma^L$ and $\Gamma_\sigma^R = \Gamma^R$, we obtain

$$I^L = I_\uparrow^L + I_\downarrow^L = \begin{cases} 2e(\Gamma^L \Gamma^R)/(2\Gamma^L + \Gamma^R), & eV > 0 \\ -2e(\Gamma^L \Gamma^R)/(2\Gamma^L + \Gamma^R), & eV < 0, \end{cases} \quad (15)$$

in accordance with results already known in the literature.³⁶

Using Eq. (14) into the definition $\varphi = (I_\uparrow - I_\downarrow)/(I_\uparrow + I_\downarrow)$, we obtain the current polarization plateau in the CB regime

$$\varphi = \frac{(\Gamma_\uparrow^\eta - \Gamma_\downarrow^\eta) \Gamma_{\bar{\sigma}}^{\bar{\eta}} \Gamma_{\bar{\sigma}}^{\bar{\eta}}}{(\Gamma_\uparrow^\eta + \Gamma_\downarrow^\eta) \Gamma_{\bar{\sigma}}^{\bar{\eta}} \Gamma_{\bar{\sigma}}^{\bar{\eta}}}, \quad (16)$$

where $\eta = L$, $\bar{\eta} = R$ for $eV > 0$ and $\eta = R$, $\bar{\eta} = L$ for $eV < 0$. We model the tunneling rates by $\Gamma_\uparrow^L = \Gamma_\downarrow^L = \Gamma_0$ and $\Gamma_{\uparrow(\downarrow)}^R = \Gamma_0(1 \pm p)$, where $p \in [0, 1]$ is the polarization degree of the ferromagnetic right lead²³ and Γ_0 the lead-dot coupling. Within this model Eq. (16) gives

$$\varphi = \begin{cases} 0, & eV > 0 \\ p, & eV < 0. \end{cases} \quad (17)$$

Thus, in the CB regime the current is unpolarized for positive bias, while spin-polarized for negative bias. Therefore the NM-QD-FM junction functions as a *current-polarization diode*.

IV. RESULTS

A. Parameters

We assume that the dot level depends on the bias voltage according to $\epsilon_d = \epsilon_{gate} - xeV$, where x accounts for asymmetric voltages drop along the left and right barriers.^{22,23} ϵ_{gate} can be controlled via gate voltages. For the numerics we take $\epsilon_{gate} = 0.5$ meV, $\mu_L = 0$, $\mu_R = -eV$, $k_B T = 212$ μ eV, $U = 3$ meV and $\Gamma_0 = 10\mu$ eV.³⁷ In Secs. B, C and D we assume a symmetric potential drop across the system with $x = 0.5$. In Sec. E we briefly discuss the asymmetric case with $x \neq 0.5$.

B. Current polarization

Figure 2 shows the current polarization as a function of the external bias eV . We observe that for positive bias the current polarization decreases for increasing bias, reaching zero around $eV = 4$ meV. Conversely, for the negative biases we obtain a maximum polarization at $eV = -4$ meV, confirming the analytical result found in Sec. III. The voltage range for this behavior scales with the parameter U . Above the Coulomb blockade ($|eV| > 7$ meV) the polarization reaches the same nonzero value. Both the suppression ($eV > 0$) and the enhancement ($eV < 0$) of the current polarization are due to the interplay of Coulomb interaction and spin accumulation in the quantum dot. Quite interestingly this interplay operates on φ differently with the bias sign, namely, for direct bias it suppresses φ while for reverse bias it enhances φ .³⁸ The suppression of φ for positive bias results in zero polarization in the Coulomb blockade regime for all p values except $p = 1$. In the half-metallic case ($p = 1$) there is only spin up current flowing in the system ($I_\uparrow^\eta \neq 0$, $I_\downarrow^\eta = 0$), so the polarization becomes simply $\varphi = (I_\uparrow^\eta - I_\downarrow^\eta)/(I_\uparrow^\eta + I_\downarrow^\eta) = I_\uparrow^\eta/I_\uparrow^\eta = 1$. On the other hand, for negative bias, the polarization φ changes in the Coulomb blockade regime as p varies. In particular, φ attains a maximum plateau equal to the polarization degree of the ferromagnetic lead [according to Eq. (17)]. To gain a more detailed understanding of the diode effect we next investigate the spin accumulation $m = n_\uparrow - n_\downarrow$ and the spin-resolved $I - V$ curves as a function of the bias.

C. Spin accumulation

Figure 3 shows the spin accumulation $m = n_\uparrow - n_\downarrow$ as a function of the bias voltage, for distinct polarization parameters p . For all the p values considered here we note that $m < 0$ for positive bias and $m > 0$ for negative bias. This spin-imbalance can be understood in terms of the tunneling rates Γ_σ^η between dot and leads. Due to the ferromagnetism of the right lead, the rates Γ_σ^L and Γ_σ^R become asymmetric. For example, for $p = 0.2$ the rates

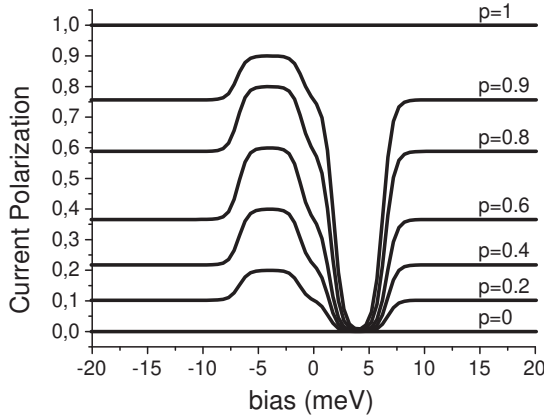


FIG. 2: Current polarization as a function of the external bias. For $p = 0$ the polarization is zero while for $p = 1$ it is one for any bias value. This means that for $p = 1$ only electrons with spin up can flow through the system, which is expected since there is no spin down states available in the right lead. For intermediate p values we observe the rectification effect: for positive bias the polarization becomes close to zero while for negative bias it presents a high value. However this effect is observed only in the Coulomb blockade regime ($|eV| < 7$ meV). For $|eV| > 7$ meV the polarization attains equal nonzero values for both bias direction.

are $\Gamma_{\uparrow}^R = 12 \mu\text{eV}$, $\Gamma_{\downarrow}^R = 8 \mu\text{eV}$ and $\Gamma_{\uparrow}^L = \Gamma_{\downarrow}^L = 10 \mu\text{eV}$. For positive bias, Γ_{σ}^L becomes the ingoing tunneling rate for electrons with spin σ and Γ_{σ}^R the outgoing tunneling rate. Due to the inequality $\Gamma_{\uparrow}^R > \Gamma_{\uparrow}^L$, the spin up electrons can tunnel out the dot faster than they come into it. On the other hand, since $\Gamma_{\downarrow}^R < \Gamma_{\downarrow}^L$, the spin down electrons leave the dot slower than they come into it. So on average the spin down electrons spend more time in the dot than the spin up ones for $eV > 0$, thus $n_{\downarrow} > n_{\uparrow}$ ($m < 0$). A similar reasoning applies to the other p values, except for $p = 0$ for which there is no accumulation. For negative bias, Γ_{\uparrow}^L and Γ_{\downarrow}^L are the outgoing tunneling rates while Γ_{\uparrow}^R and Γ_{\downarrow}^R become the ingoing tunneling rates. As a consequence of this interchange, the spin accumulation inverts its sign ($m > 0$). For small p values the spin accumulation is essentially an odd function of the bias. When p increases, though, the imbalance becomes stronger for positive bias. In particular for $p = 1$, m reaches -1 in the Coulomb blockade regime for positive bias and a constant plateau for negative bias. This happens because no spin-down states are available in the right lead for $p = 1$, so a spin-down electron that enters the dot, coming from the left lead ($eV > 0$), cannot leave the dot to the right lead. In addition, a spin-up electron cannot hop into the dot due to the Coulomb blockade so the accumulation becomes completely spin-down polarized for positive bias. For biases above the Coulomb blockade an additional electron with opposite spin can

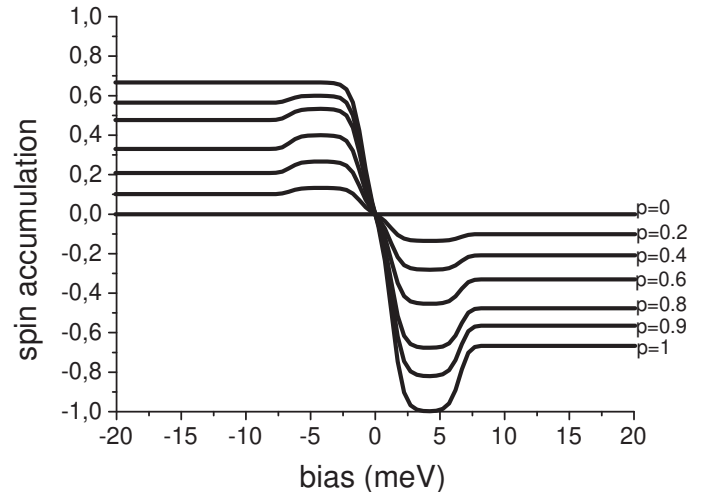


FIG. 3: Spin accumulation $m = n_{\uparrow} - n_{\downarrow}$ as a function of the external bias. For $p = 0$ (unpolarized lead) there is no spin accumulation in the dot. When p increases the spin accumulation increases as well; m becomes more negative for $eV > 0$ than positive for $eV < 0$ with increasing p . In particular for $p = 1$, the spin accumulation reaches one in the Coulomb blockade regime for $eV > 0$. This means that the dot becomes fully spin-down polarized.

jump into the dot (for both positive and negative bias) thus resulting in a suppression (in modulus) of m .

D. Spin-resolved currents

In figure 4 we show the spin resolved currents I_{\uparrow} and I_{\downarrow} as a function of the bias voltage for differing polarization parameters p . We observe that for positive bias the spin up and spin down current plateaus coincide in the Coulomb blockade regime for any p value (indicated by arrows). This results in the zero current-polarization seen in Fig. 2. Above the Coulomb blockade ($eV > 7$ meV) I_{\uparrow} attains higher values compared with I_{\downarrow} which enhances φ . The strong suppression of I_{\uparrow} in the Coulomb blockade regime is attributed to the spin imbalance $m < 0$ observed for $eV > 0$. More specifically, since the dot is predominantly spin-down occupied for positive bias, the spin-up electrons tend to be more blocked than the spin-down ones, thus reducing further I_{\uparrow} and eventually putting it on top of I_{\downarrow} . In contrast, for negative bias we have the population inversion $m > 0$. This gives a stronger suppression of I_{\downarrow} as compared to I_{\uparrow} , which enhances the difference between I_{\uparrow} and I_{\downarrow} , and consequently φ . Above the CB ($eV < -7$ meV) both the I_{\uparrow} and I_{\downarrow} plateaus attain values somewhat closer to each other, thus reducing the current polarization (see Fig. 2).

In particular for $p = 1$ the I_{\downarrow} is zero for any bias voltage since there are no spin-down states available in the right lead. The I_{\uparrow} increases slightly (for positive bias) while

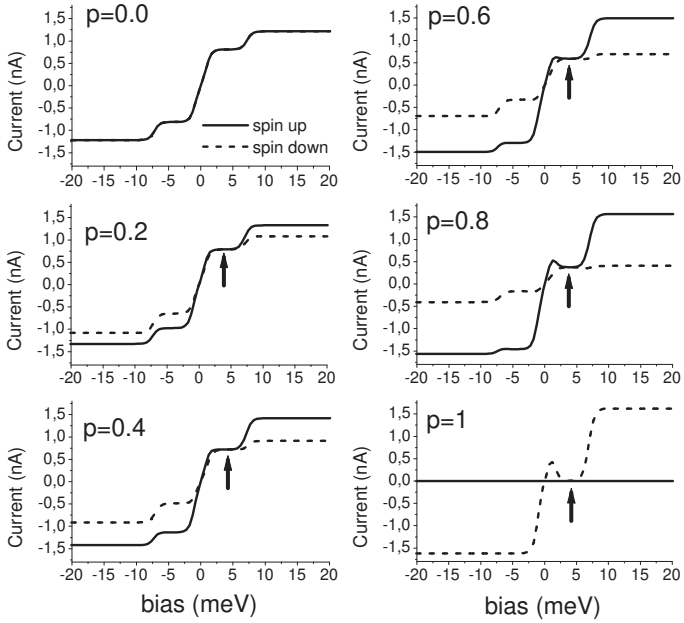


FIG. 4: Spin-resolved currents against bias voltage. Note that I_{\uparrow} lies on top of I_{\downarrow} in the Coulomb blockade regime, due to the strong suppression of I_{\uparrow} in this regime. In contrast, for negative bias the CB tends to suppress strongly I_{\downarrow} which enhances the difference $I_{\uparrow} - I_{\downarrow}$ resulting in an enhancement of the current polarization.

the dot is becoming populated. When the population is high enough the Coulomb blockade takes place and the I_{\uparrow} goes down to zero.³⁹ This gives rise to a negative differential conductance at the beginning of the CB plateau for $eV > 0$ [see Fig. (4) with $p = 1$]. For negative bias (and $p = 1$) I_{\uparrow} attains one plateau instead of two steps as for the others p values. This is expected because the spin-down electrons do not participate in the transport in this case, so no Coulomb blockade effect arises. Note that for $p = 1$ the system can work as a mesoscopic current diode.^{4,31,32}

E. Effects of the bias-drop asymmetry

Here we consider the effects of an asymmetric bias drop, i.e., $x \neq 0.5$. As Fig. 5 shows, the asymmetry in the bias drop gives rise to quantitative, but not qualitative changes. For $x = 0.2$ the current polarization φ goes to zero much slower with the bias than it does for $x = 0.5$. This is so because the resonance condition $\epsilon_d \leq \mu_L$ ($eV > 0$), which is necessary to have $\varphi = 0$ [see Sec.(III)], happens for higher bias when x decreases. For negative bias the resonance $\epsilon_d \leq \mu_R$ is reached faster (i.e., at lower biases as compared with the $x = 0.5$ case) for decreasing x . This, in turn, translates into a steeper enhancement of φ which then attains a plateau at $\varphi = p$ [see Eq. (17)]. In addition, for $x = 0.2$ the plateau shrinks

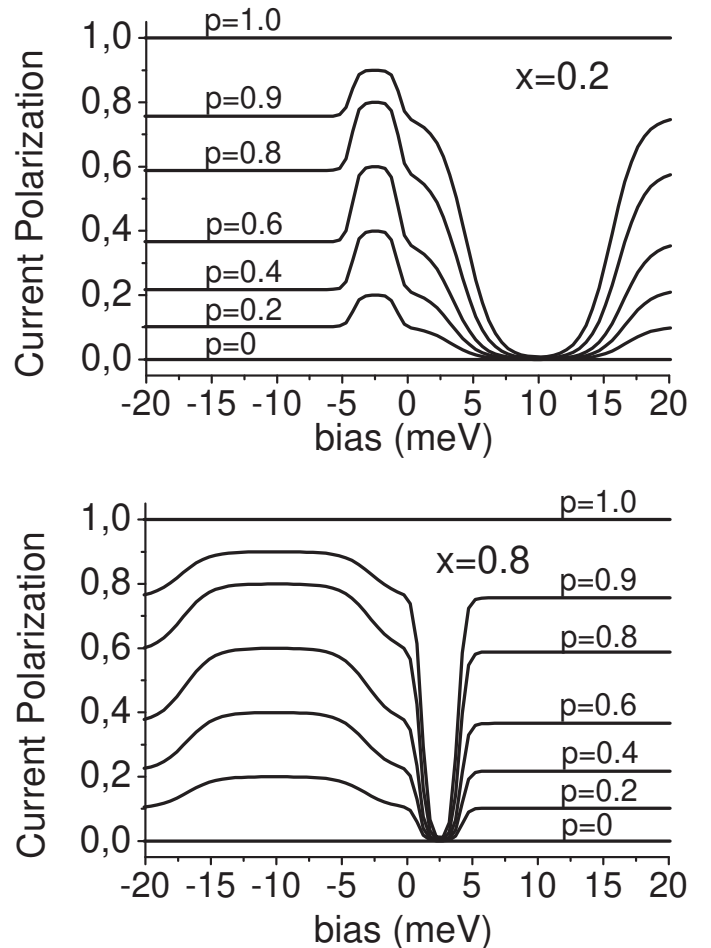


FIG. 5: Current polarization as a function of the bias voltage for the asymmetry parameters (a) $x = 0.2$ and (b) $x = 0.8$. For $x = 0.2$ the level ϵ_d follows slowly the bias voltage eV , while for $x = 0.8$ it moves faster with eV . So for positive bias the resonances $\epsilon_d = \mu_L$ and $\epsilon_d + U = \mu_L$ happen faster for $x = 0.8$ than for $x = 0.2$. This in turn makes the $\varphi = 0$ plateau wide for $x = 0.2$ and narrow for $x = 0.8$. In contrast, for negative biases the matches $\epsilon_d = \mu_R$ and $\epsilon_d + U = \mu_R$ are faster with eV for $x = 0.2$ than for $x = 0.8$, thus resulting in a shrinkage of the $\varphi = p$ plateau for $x = 0.2$ and in an enlargement of this plateau for $x = 0.8$.

compared to its $x = 0.5$ width. For $x = 0.8$ the resonance $\epsilon_d \leq \mu_L$ ($eV > 0$) takes place faster with the bias when compared to the $x = 0.2$ and $x = 0.5$ cases. This results in the steeper suppression of φ and the shrinkage of the zero-polarization bias range. For negative biases the resonance condition $\epsilon_d \leq \mu_R$ for $x = 0.8$ is more slowly attained with the bias as compared to the $x = 0.2$ and $x = 0.8$ cases. Consequently, the polarization φ reaches the plateau at $\varphi = p$ for high bias voltages (in modulus).

V. CONCLUSION

We propose a system (NM-QD-FM) which operates as a diode for the current polarization. More specifically, in the CB regime our system yields an unpolarized current for positive bias and a spin-polarized current for negative bias. This effect is a result of the interplay between spin accumulation in the dot and the Coulomb blockade effect. Interestingly, for positive biases the spin-resolved currents are essentially equal to each other due to the spin-dependent CB effect, which yields $\varphi = 0$ in this regime. Nonequilibrium Green functions with suitable approximations were also used to corroborate the master equation results.

The authors acknowledge G. Platero, K. Flensberg and T. Novotný for helpful comments. JCE acknowledges support from CNPq and FAPESP.

APPENDIX A: NONEQUILIBRIUM GREEN FUNCTIONS

In the main text we have formulated the problem via master equation formalism. An alternative description is provided by the nonequilibrium Green function technique, which gives similar results when $k_B T \gg \Gamma_0$ and the perturbation expansion is approximated at the Hartree-Fock level. We start with the well known equation for the current^{40,41}

$$I_\sigma^\eta = ie \int \frac{d\epsilon}{2\pi} \{ \Gamma_\sigma^\eta \{ [G_{\sigma\sigma}^r(\epsilon) - G_{\sigma\sigma}^a(\epsilon)] f_\eta(\epsilon) + G_{\sigma\sigma}^<(\epsilon) \} \}, \quad (\text{A1})$$

where $G_{\sigma\sigma}^r$, $G_{\sigma\sigma}^a$ and $G_{\sigma\sigma}^<$ are the retarded, advanced and lesser Green functions, respectively. To calculate them we apply the equation of motion technique and use the Hartree-Fock approximation to factorize high-order correlation functions in the resulting chain of equations.⁴² The retarded Green function becomes

$$G_{\sigma\sigma}^r(\epsilon) = \frac{1}{g_{\sigma\sigma}^{-1}(\epsilon) - \Sigma_\sigma^r(\epsilon)}, \quad (\text{A2})$$

where $\Sigma_\sigma^r(\epsilon)$ is the non-interacting tunneling self-energy given in the wide band approximation (WBA) by $\Sigma_\sigma^r(\epsilon) = -i\Gamma_\sigma/2 = -i(\Gamma_\sigma^L + \Gamma_\sigma^R)/2$, and $g_{\sigma\sigma}(\epsilon)$ is the dot Green function without coupling to leads,

$$g_{\sigma\sigma}(\epsilon) = \frac{\epsilon - \epsilon_d - U(1 - n_{\bar{\sigma}})}{(\epsilon - \epsilon_d)(\epsilon - \epsilon_d - U)}, \quad (\text{A3})$$

where $n_{\bar{\sigma}}$ is the dot occupation number, with $\bar{\sigma} = -\sigma$. This occupation can be calculated self-consistently via

$$n_\sigma = \langle d_\sigma^\dagger d_\sigma \rangle = -i \int \frac{d\epsilon}{2\pi} G_{\sigma\sigma}^<(\epsilon), \quad (\text{A4})$$

where the correlation function $G_{\sigma\sigma}^<(\epsilon)$ is given by the Keldysh equation

$$G_{\sigma\sigma}^<(\epsilon) = G_{\sigma\sigma}^r(\epsilon) \Sigma_\sigma^< G_{\sigma\sigma}^a(\epsilon). \quad (\text{A5})$$

The advanced Green function $G_{\sigma\sigma}^a(\epsilon)$ is given by $G_{\sigma\sigma}^a(\epsilon) = [G_{\sigma\sigma}^r(\epsilon)]^*$, while $\Sigma_\sigma^< = i[\Gamma_\sigma^L f_L + \Gamma_\sigma^R f_R]$. Substituting the Green functions into Eq. (A1) and solving the problem in a self-consistent way we obtain numerical results which are almost indistinguishable from the ones presented in Figs. 2 - 5, in the parameter range considered. Interestingly, in the large- U limit we can find analytical results that coincide with Eqs. (13) and (14). In this limit the retarded Green function can be approximated by

$$G_{\sigma\sigma}^r(\epsilon) = \frac{(1 - n_{\bar{\sigma}})}{\epsilon - \epsilon_d - \Sigma_\sigma^r(1 - n_{\bar{\sigma}})}. \quad (\text{A6})$$

The lesser Green function becomes

$$G_{\sigma\sigma}^<(\epsilon) = \frac{i(\Gamma_\sigma^L f_L + \Gamma_\sigma^R f_R)(1 - n_{\bar{\sigma}})^2}{(\epsilon - \epsilon_d)^2 + (\frac{\Gamma_\sigma}{2})^2(1 - n_{\bar{\sigma}})^2}. \quad (\text{A7})$$

Substituting Eq. (A7) into Eq. (A4) we have

$$n_\sigma = \frac{(1 - n_{\bar{\sigma}})^2}{2\pi} \int d\epsilon \frac{(\Gamma_\sigma^L f_L + \Gamma_\sigma^R f_R)}{(\epsilon - \epsilon_d)^2 + (\frac{\Gamma_\sigma}{2})^2(1 - n_{\bar{\sigma}})^2}. \quad (\text{A8})$$

Now assuming that the dot level ϵ_d is completely on resonance within the conduction window between μ_L and μ_R for positive or negative bias⁴³ we can integrate Eq. (A8) in order to obtain exactly Eq. (13).

We can also determine the spin-resolved current analytically from the Green functions. Substituting Eqs. (A6) and (A7) into the current expression (A1) we reach the integral

$$I_\sigma^L = -e \int \frac{d\epsilon}{2\pi} \frac{\Gamma_\sigma^L \Gamma_\sigma^R (1 - n_{\bar{\sigma}})^2 (f_R - f_L)}{(\epsilon - \epsilon_d)^2 + (\frac{\Gamma_\sigma}{2})^2(1 - n_{\bar{\sigma}})^2}, \quad (\text{A9})$$

which when solved with the same assumptions adopted previously⁴³ we find precisely Eq. (14).

¹ For an overview see e.g. *Semiconductor Spintronics and Quantum Computation*, eds. D. D. Awschalom, D. Loss, and N. Samarth, Springer, Berlin, 2002; I. Zutic, J. Fabian, and S. Das Sarma, Rev. Mod. Phys. **76**, 323 (2004).

² D. Loss and D. P. DiVincenzo, Phys. Rev. A **57**, 120 (1998).

³ H.-A. Engel, P. Recher, and D. Loss, Sol. State Comm. **119**, 229 (2001).

⁴ M. Wilczyński *et al.*, J. Magn. Magn. Mater. **290-291**, 209 (2005).

⁵ R. Świrkowicz, M. Wilczyński, and J. Barnaś, Phys. Rev. B **73**, 193312 (2006).

⁶ J. Martinek *et al.*, Phys. Rev. B **72**, 121302(R) (2005).

⁷ Y. Utsumi *et al.*, Phys. Rev. B **71**, 245116 (2005).

⁸ J. Martinek *et al.*, Phys. Rev. Lett. **91**, 127203 (2003).

⁹ P. Zhang, Q.-K. Xue, Y. Wang, and X. C. Xie, Phys. Rev. Lett. **89**, 286803 (2002).

¹⁰ F. Elste and C. Timm, Phys. Rev. B **73**, 235305 (2006).

¹¹ I. Weymann *et al.*, Phys. Rev. B **72**, 113301 (2005).

¹² A. Cottet, W. Belzig, and C. Bruder, Phys. Rev. Lett. **92**, 206801 (2004); A. Cottet and W. Belzig, Europhys. Lett. **66** (3), 405 (2004).

¹³ J. Barnaś and A. Fert, Phys. Rev. Lett. **80**, 1058 (1998).

¹⁴ S. Takahashi and S. Maekawa, Phys. Rev. Lett. **80**, 1758 (1998).

¹⁵ K. Walczak and G. Platero, CEJP 4(1), 30 (2006).

¹⁶ I. Weymann and J. Barnaś, Phys. Rev. B **73**, 33409 (2006).

¹⁷ J. Varalda *et al.*, Phys. Rev. B **72**, 81302(R) (2005).

¹⁸ I. Weymann *et al.*, Phys. Rev. B **72**, 115334 (2005).

¹⁹ F. M. Souza, J. C. Egues, and A. P. Jauho, Braz. J. Phys. **34**, 565 (2004).

²⁰ R. López and D. Sánchez, Phys. Rev. Lett. **90**, 116602 (2003).

²¹ I. Weymann and J. Barnaś, Phys. Stat. Sol. (b) **236**, 651 (2003).

²² W. Rudziński, J. Barnaś, and M. Jankowska, J. Mag. Mag. Mater. **261**, 319 (2003).

²³ W. Rudziński and J. Barnaś, Phys. Rev. B **64**, 85318 (2001).

²⁴ P. Recher, E. V. Sukhorukov, and D. Loss Phys. Rev. Lett. **85**, 1962 (2000);

²⁵ H.-A. Engel and D. Loss Phys. Rev. B **65**, 195321 (2002);

²⁶ E. Cota, R. Aguado, and G. Platero, Phys. Rev. Lett. **94**, 107202 (2005).

²⁷ J. Martinek *et al.*, Phys. Rev. B **66**, 14402 (2002).

²⁸ H. Imamura, S. Takahashi, and S. Maekawa, Phys. Rev. B **59**, 6017 (1999).

²⁹ J. Wang, K. S. Chan, and D. Y. Xing, Phys. Rev. B **72**, 115311 (2005).

³⁰ W. Kuo and C. D. Chen, Phys. Rev. B **65**, 104427 (2002).

³¹ I. Weymann and J. Barnaś, Phys. Rev. B **73**, 205309 (2006).

³² R. Świrkowicz *et al.*, J. Magn. Magn. Mater. **272-276**, 1959 (2004).

³³ H. Dalgleish and G. Kirczenow, Phys. Rev. B **73**, 235436 (2006).

³⁴ A. A. Shokri, M. Mardaani, and K. Esfarjani, Physica E **27**, 325 (2005)

³⁵ L. I. Glazman and K. A. Matveev, JEPT Lett. **48**, 445 (1988).

³⁶ See, for example, A. Thielmann *et al.*, Phys. Rev. B **68**, 115105 (2003), and Y. V. Nazarov and J. J. R. Struben, Phys. Rev. B **53**, 15466 (1996).

³⁷ Typical values of Γ_0 and U can be found in, for example, A. Kogan *et al.*, Phys. Rev. Lett. **93**, 166602 (2004); F. Simmel *et al.* Phys. Rev. Lett. **83**, 804 (1999); D. Goldhaber-Gordon *et al.*, Nature **391**, 156 (1998).

³⁸ For a system with two ferromagnetic leads coupled to a quantum dot (FM-QD-FM), it is possible to have an enhancement of φ for negative biases and a suppression of φ for positive biases when the lead magnetizations are aligned antiparallel. However, the polarization does not vanish for any particular bias range and consequently no rectification effect is observed - F. M. Souza, PhD thesis, University of São Paulo, Brazil (2004).

³⁹ A similar bump in the total current ($I_\uparrow + I_\downarrow$) was already predicted in B. R. Bulka, Phys. Rev. B **62**, 1186 (2000), and also in [4], [22] and [23].

⁴⁰ Y. Meir and N. S. Wingreen, Phys. Rev. Lett. **68**, 2512 (1992).

⁴¹ A. P. Jauho, N. S. Wingreen, and Y. Meir, Phys. Rev. B **50**, 5528 (1994).

⁴² H. Haug and A. P. Jauho, Quantum Kinetics in Transport and Optics of Semiconductors, Springer Solid-State Sciences **123** (1996).

⁴³ More precisely we assume that $\mu_R < \epsilon_d < \mu_L$ for $eV > 0$ and $\mu_L < \epsilon_d < \mu_R$ for $eV < 0$. In addition we approximate $f_L \approx 1$ and $f_R \approx 0$ for $eV > 0$ and $f_L \approx 0$ and $f_R \approx 1$ for $eV < 0$.